Journal of Atmospheric and Solar-Terrestrial Physics ▮ (▮▮▮▮) ▮▮▮–▮▮▮

Contents lists available at ScienceDirect

Journal of Atmospheric and Solar-Terrestrial Physics

journal homepage: www.elsevier.com/locate/jastp

Stereoscopic analysis of STEREO/SECCHI data for CME trajectory determination

P.C. Liewer [a,*], J.R. Hall [a], R.A Howard [b], E.M. De Jong [a], W.T Thompson [c], A. Thernisien [d]

[a] Jet Propulsion Laboratory, California Institute of Technology, MS 169-506, Pasadena, CA 91109, USA
[b] Naval Research Laboratory, Washington, DC 20375, USA
[c] Adnet Systems, Inc., Lanham, MD 20706, USA
[d] Universities of Space Research Association, Columbia, MD 21044, USA

ARTICLE INFO

Article history:
Received 30 March 2010
Received in revised form
31 August 2010
Accepted 3 September 2010

Keywords:
Coronal mass ejections
Stereoscopy
STEREO

ABSTRACT

The *Sun Earth Connection Coronal and Heliospheric Investigation* (SECCHI) coronagraphs on the twin *Solar TErrestrial RElations Observatory* (STEREO) spacecraft provide simultaneous views of the corona and coronal mass ejections from two view points. Here, we analyze simultaneous image pairs using the technique of tie-pointing and triangulation (T&T) to determine the three-dimensional trajectory of seven coronal mass ejections (CMEs). The bright leading edge of a CME seen in coronagraph images results from line-of-sight integration through the CME front; the two STEREO coronagraphs see different apparent leading edges, leading to a systematic error in its three-dimensional reconstruction. We analyze this systematic error using a simple geometric model of a CME front. We validate the technique and analysis by comparing T&T trajectory determinations for seven CMEs with trajectories determined by Thernisien et al. (2009) using a forward modeling technique not susceptible to this systematic effect. We find that, for the range of spacecraft separation studied ($\leq 50^\circ$), T&T gives reliable trajectories (uncertainty $<10^\circ$ in direction and $<15\%$ velocity) for CME propagating within approximately $\pm 40^\circ$ of perpendicular to Sun–Earth line. For CMEs close to the Sun–Earth or Sun–Spacecraft lines, T&T is subject to larger errors, especially in the velocity.

1. Introduction

Coronal mass ejections (CMEs) are a major contributor to "space weather", just as storms are major contributors to Earth's weather (Luhman, 1997; Baker, 2000; Srivastava and Venkatakrishnan, 2004). CMEs that impact Earth's magnetosphere can cause severe geomagnetic storms and enhanced radiation belts. CME-associated energetic particles can damage spacecraft throughout the solar system. Understanding CMEs and their evolution in the heliosphere is necessary to develop a predictive capability for space weather. The solar observations from the SOlar and Heliospheric Observatory (SOHO) led to a tremendous advance in our understanding of CMEs and their origins (see Cremedas and Bothmer, 2004 and references therein). However, with only one viewpoint, only incomplete knowledge of a CME source region and trajectory could be obtained. Foremost, one viewpoint only gives a "plane-of-sky" (POS) projection of the CME's trajectory so it is not possible to determine the CME's propagation angle with respect to the Sun–Earth line. This is especially critical for Earth-directed "halo" CMEs: Although the source region (presumably somewhere near disk center) can be observed from Earth, the propagation angle is poorly determined by the POS projection. In addition, with only the single Earth viewpoint, the source region of "limb CMEs," e.g., CMEs propagating nearly perpendicular to the Sun–Earth line, cannot be well observed. The launch of the twin *Solar TErrestrial RElations Observatory* (STEREO) spacecraft (Kaiser, 2005) in October 2006 has provided simultaneous observations of the solar atmosphere from two vantage points. These two simultaneous observations provide information on the three-dimensional (3D) trajectory of CMEs and better information on the location of the CME source regions. Both are important to advance our ability to predict space weather. This paper focuses on the 3D trajectory determination using stereoscopy.

The twin STEREO spacecraft are in approximately 1 AU heliocentric orbits. The STEREO A spacecraft drifts ahead of Earth while the STEREO B spacecraft lags behind, each spacecraft separating from the Earth at about 22°/year (Kaiser, 2005). The spacecraft carry remote sensing and *in situ* instrument suites. The *Sun Earth Connection Coronal and Heliospheric Investigation* (SECCHI) imaging package on each spacecraft includes five telescopes: an Extreme Ultra Violet Imager (EUVI), two white-light coronagraphs (COR1 and COR2), and two white-light heliospheric imagers (HI1 and HI2) (Howard et al., 2007). Most of the results in this paper are obtained from analysis of data from the two white-light coronagraphs: COR1 covers the region from 1.4 to 4 R_S (solar radii); COR2 covers the regions from 2.5 to

* Corresponding author. Fax: +1 818 354 8895.
E-mail address: paulett.liewer@jpl.nasa.gov (P.C. Liewer).

1364-6826/$ - see front matter © 2010 Published by Elsevier Ltd.
doi:10.1016/j.jastp.2010.09.004

15 R_S. We also use information from SECCHI's HI1 telescope, which overlaps with the COR2 field-of-view at the outer edge; HI1 has a 20° field-of-view covering the sky from about 4° to 24° from the Sun. The separation between the two spacecraft ranged from 28° to 50° for the data analyzed here. SECCHI data is available through the STEREO Science Center (http://stereo-ssc.nascom.nasa.gov).

Several techniques have been developed to analyze the STEREO data and determine the 3D trajectories of CMEs seen by both spacecraft (Mierla et al., 2008; Thernisien et al., 2009; Mierla et al., 2009, Srivastava et al., 2009; Maloney et al., 2009; Temmer et al., 2009; Colaninno and Vourlidas, 2009; Liewer et al., 2009b). These and other techniques have been reviewed by Mierla et al. (2010). The bright leading edge of a CME seen in coronagraph images results from line-of-sight integration through the optically thin CME. As noted in Mierla et al. (2010), depending on the separation angle, the two STEREO spacecraft may see significantly different apparent leading edges of the CME, which leads to an error in its three-dimensional reconstruction. We call this the different-apparent-leading-edge (DALE) effect. In this paper, we expand on the results in Liewer et al. (2009b), presenting results using tie-pointing and triangulation (T&T) to determine CMEs trajectories and we use a simple model to analyze the error caused by the DALE effect. Depending on the viewing geometry, the error in the velocity and/or propagation direction caused by the DALE effect can be quite large and allowances must be made for this error if the technique is to be used as a predictive tool. We validate the technique and analysis by comparing T&T trajectory determinations for seven CMEs with determinations by Thernisienst al. (2009, TVH hereafter) who use a forward modeling technique not susceptible to the DALE effect. Trajectory propagation angles are also compared with the locations of the solar source regions both as a check on the trajectory and to look for deviations of the trajectory from pure radial propagation. For one case, the T&T technique is used to measure the deflection in longitude of a CME as it propagates through the coronagraph field-of-view. We also use information from the CME's track in HI1 images to further analyze the trajectory using techniques first introduced by Sheeley et al. (1999). This allows a study of the propagation of CMEs further out into the heliosphere, where interactions with the solar wind become apparent. The technique used here is related to that used by Maloney et al. (2009) in that both use the trajectories determined stereoscopically from the coronagraph data to help analyze the CME trajectory as seen in the heliospheric imager data from one spacecraft.

The method and tool used for T&T is discussed in Section 2.1. The application of the technique to optically thin CMEs is discussed in Section 2.2. In Section 2.3, an approximate error in the trajectory determination resulting from tie-pointing different apparent leading edges (the DALE effect) is calculated using a simple hemispherical shell CME model. In Section 3, results for seven CME trajectories determined using T&T are presented and compared with the source region locations and the trajectories determined by TVH. The estimated errors from the DALE effect are also given. In Section 4, the propagation of two CMEs in the HI1 field-of-view is compared with the predicted propagation based on the trajectory information determined by T&T, using data from the coronagraph's fields-of-view, to study the propagation of the CMEs out into the heliosphere. Section 5 contains a summary and discussion of the results. The derivation of the approximate systematic error due to the DALE effect is given in Appendix.

2. Stereoscopic data analysis technique

2.1. Description of method

The two separated views of the solar atmosphere provided by the twin STEREO A (Ahead) and B (Behind) spacecraft provide the opportunity to use T&T to determine the 3D location of features observed by both spacecraft. A feature's location is marked in both images of a simultaneous pair (tie-pointing); the position of the feature in a three-dimensional heliocentric coordinate system is then determined by triangulation. The T&T procedure requires knowledge of the location and separation of the two STEREO spacecraft, as well as the relevant camera information. The headers of the SECCHI image files contain all of the information on spacecraft location, pointing (relative to the Sun) and plate scale (to convert pixel location to degrees) to the accuracy needed for 3D reconstruction (see Aschwanden et al., 2008). This technique and its application to the 3D reconstruction of an erupting solar filament was discussed in Liewer et al. (2009a). The T&T technique has been used by others for 3D reconstruction of coronal loops and filaments from EUVI stereoscopic image pairs (Feng et al., 2007; Aschwanden et al., 2008) and on CMEs (Srivastava et al., 2009; Temmer et al., 2009; Maloney et al., 2009; Mierla et al., 2009).

The tool used here and in Liewer et al. (2009a,b), called `sunloop`, is available in the SECCHI software library distributed as part of the SolarSoft suite (http://www.lmsal.com/solarsoft/). Illustration of the use of the `sunloop` tool for the 3D reconstruction and visualization of coronal loops and prominences can be found in Liewer et al. (2009a). For analysis of CMEs, the images are first processed using the `secchi_prep` routine, also part of the SECCHI SolarSoft library, to produce total brightness images. Slowly varying (monthly minimum) backgrounds are subtracted; this removes the F-corona, but not the coronal streamers. The `sunloop`tool also scales the images to correct for the different distances of the two spacecraft from the Sun to make the plate scales identical. This tool, along with the other tie-pointing methods applied to STEREO observations referenced above, makes use of the epipolar constraint: The point in the corona to be triangulated plus the two spacecraft define a plane called the epipolar plane (Inhester, 2006; also Srivastava et al., 2009), and thus all epipolar planes share the line connecting STEREO A and B (the STEREO baseline). Any point identified on a certain epipolar line in one image must lie on the same epipolar line in the other image, thus reducing the problem of placing the second tie-point from a two-dimensional to one-dimensional problem. In `sunloop`, the images are rotated to align them with the STEREO baseline so that the epipolar lines coincide with rows in the images. Therefore two tie-points for a given feature must lie in the same row (but different columns) in both images. The `sunloop` tool also has an option to call `scc_measure`, a T&T routine developed by W.T. Thompson, to facilitate comparison of results. `Sunloop` calls the SECCHI SolarSoft routine `scc_triangulate` to perform the triangulation calculation. Tie-points are placed in each image using a cursor. Each position on an image defines a camera ray; the rays defined by the tie-points lie in an epipolar plane and, using triangulation, the location of the tie-pointed feature is the intersection of the two rays.

Results in this paper are given in the Stonyhurst heliographic (STYH) coordinate system (Thompson, 2006). In this system, the z-axis coincides with the solar rotation axis, the solar equator defines the x–y plane and the Earth lies is the x–z plane. Thus the coordinate system rotates with Earth, but the STYH latitude of Earth varies in time due to the relative tilt between the solar equatorial and ecliptic planes. Longitude, measured from the x-axis, is 0° for Earth and ranges between −180° and +180° where positive increases towards the Sun's west limb; latitude increases toward the solar north pole at 90° latitude. This system is very closely related to the Carrington coordinate system; it differs only in a time-dependent offset in longitude (Thompson, 2006). The STYH system is also closely related to the Cartesian Heliocentric Earth Equatorial (HEEQ) coordinate system (Thompson, 2006).

Please cite this article as: Liewer, P.C., et al., Stereoscopic analysis of STEREO/SECCHI data for CME trajectory determination. Journal of Atmospheric and Solar-Terrestrial Physics (2010), doi:10.1016/j.jastp.2010.09.004

2.2. Application of T&T to CMEs

To determine a CME trajectory, the leading edge of the CME is reconstructed using T&T at multiple times (multiple simultaneous pairs). Here and in Liewer et al. (2009b), the term "CME trajectory" refers to the velocity and direction of propagation of the "apex" of the CME front, generally the point on the CME front most distant from the Sun. We illustrate the T&T technique using the CME of 25 March 2008. Fig. 1 shows the window of the `sunloop` tool with the CME front as seen in COR2 at 20:08 UT with the COR2B (A) image on the left (right); tie-points are also shown. A thin leading edge is seen from both spacecraft (more easily seen on a computer screen). The tie-points were placed by locating manually the corresponding features along the CME leading edge in each image of the simultaneous pair, subject to the epipolar constraint as discussed above. The 3D leading edge reconstruction from these tie-points along with 3D reconstructions from four other times are shown in Fig. 2 from two different viewpoints in the solar equatorial plane in relation to the Sun (the 3D globe), using `sunloop`'s visualization tool `animator`. Each colored curve is a 3D reconstruction of the leading edge at one time, created from the reconstructed points. The first reconstruction (magenta) is from a COR1 image pair at 19:05 UT; the other four are from COR2 image pairs from 19:38 to 21:08 with a 30 min cadence. The three colored straight lines (here, and in other figures showing 3D reconstructions) show the directions to STEREO B (violet), Earth (green), and STEREO A (red). The points obtained by triangulation are connected with straight-line segments to visualize the 3D reconstructions of the leading edge. The trajectory determination is done using these points directly; the points are neither smoothed nor fitted to a curve. The view from Earth is shown on the left. From the viewpoint on the right in Fig. 2 (looking along the longitude of propagation), it can be seen that the CME leading edge reconstructions at the five times fall in a narrow range of longitudes. From the set of leading edge reconstructions, the trajectory is determined by selecting, at each time, the point on the reconstructed edge furthest from the Sun (the apex of the front). The trajectory propagation direction is the

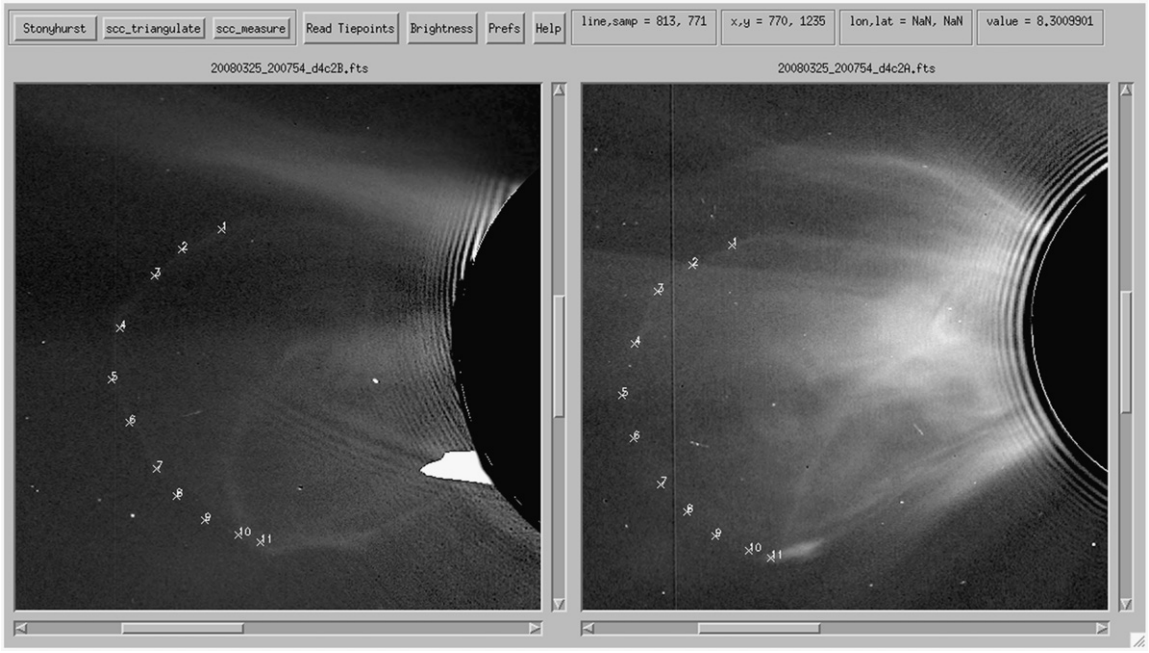

Fig. 1. The window for `sunloop` tie-pointing tool showing the placement of tie-points on the leading edge of the CME of 25 March 2008 at 20:08 UT. The COR2B (A) image is on the left (right). A well-defined (but faint) CME edge was visible in both images.

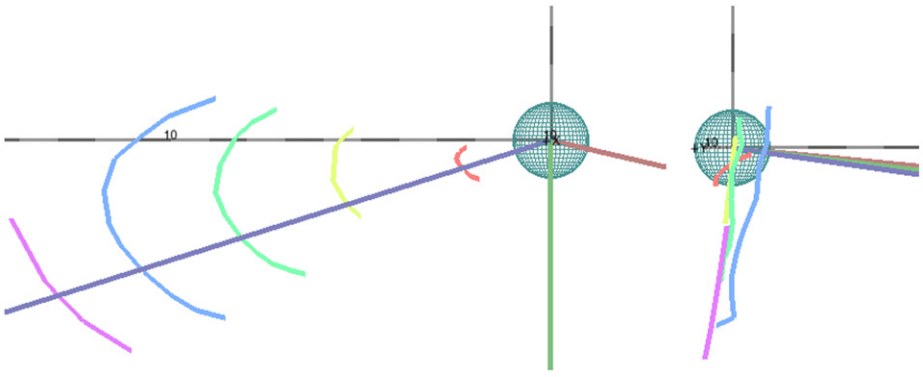

Fig. 2. 3D reconstructions of the leading edge of the CME of 25 March 2008 at five times shown in relation to the Sun (3D globe) from two views in the solar equatorial plane. The third (green) reconstruction from the Sun is from the COR2 tie-points in Fig. 1. The viewpoint on the right is approximately along the propagation longitude. The three straight lines show the directions to Earth (green), STEREO B (violet) and STEREO A (red).

Please cite this article as: Liewer, P.C., et al., Stereoscopic analysis of STEREO/SECCHI data for CME trajectory determination. Journal of Atmospheric and Solar-Terrestrial Physics (2010), doi:10.1016/j.jastp.2010.09.004

average over the directions from the Sun to the apex for each reconstruction; the velocity is obtained from a linear fit to the true (3D) distance versus time data.

CMEs are optically thin structures scattering sunlight over an extended volume via Thomson scattering from electrons. The brightness at a given point in image is a result of line-of-sight integrated scattered signal. What is seen as the bright front in the white light images thus represents the integrated signal along the line-of-sight passing through the CME volume. Because of different viewing geometries and different lines of sight, two SC will see different apparent leading edges (DALE). The error introduced by the DALE effect is analyzed in next section. Other features such as corona streamers that lie along the line-of-sight will also contribute to the scattering signal and thus are an additional source of error in tie-point placement.

Another aspect of Thomson scattering also contributes errors in reconstruction from coronagraph images. The Thomson scattered signal from a volume element depends on the electron density and on Ω, the observer–electron–Sun angle, with the scattering maximized for $\Omega=90^\circ$ (Billings, 1966). The locus of points with $\Omega=90^\circ$ defines the Thomson sphere for each observer (A, B or Earth). The scattered total brightness signal strength falls off gradually away from the surface of the sphere, falling to about half maximum when $\Omega \approx 90^\circ \pm 30^\circ$ and to zero for $\Omega=0^\circ$ and 180° (on the observer–Sun line) (Hundhausen, 1993). The brightness of a CME front will therefore also depend on its distance from the Thomson sphere. Thus it may be difficult to identify the leading edge of a CME if it is far from the Thomson sphere, leading to further uncertainly in placing tie-points. For coronagraphs with narrow fields of view (angular size $\ll \pi/2$), the Thomson sphere can be approximated as the more familiar "plane-of-sky," but for large fields of view such as STEREO's Heliospheric Imagers, Thomson sphere effects on the viewing of CMEs become important (Vourlidas and Howard, 2006).

2.3. Analysis of error CME trajectory due to DALE effect

There are various sources of error for 3D reconstruction from coronagraph images, as discussed above (see also Mierla et al., 2010), resulting from the fact that CMEs are optically thin structures. Here we analyze only the systematic error in the trajectory determination introduced by the DALE effect, which is unique to the T&T technique and which adds to the other sources of error. Since the two spacecraft see different apparent leading edges, it is not the same physical points that are being tie-pointed along the CME leading edge. To analyze the resulting error, we introduce a simple infinitely thin hemispherical shell model of a CME of radius a with sphere–center distance R from the Sun. The CME density is uniform on the thin shell and zero elsewhere. We use this model only to calculate this systematic error from the DALE effect; it is not used to determine the CME trajectories. Note that the errors we calculate depend on the assumed geometry of our simple model and so the DALE-effect errors should be considered approximate.

The CME is assumed to propagate in the ecliptic plane at an angle β with respect to the Sun–Earth line. Fig. 3 (left) shows the geometry for the case when the propagation angle β is larger than θ, the angle between Earth and Spacecraft A; Fig. 3 (right) shows the small propagation angle geometry ($\beta<\theta$). The brightest features in the white light image will result from lines-of-sight with the longest path length through the thin shell since those have the largest integrated electron density and thus scattering signal (assuming Thomson sphere effects are negligible). These will be the rays tangent to hemispherical shell, which, for a camera at infinity, are rays parallel to the direction to the spacecraft as shown in Fig. 3. Note that in the small angle case, the tangent rays from the brightest features come from opposite sides of the CME front.

When the T&T technique is applied to a CME viewed from two separated spacecraft, and if the brightest leading edges are tie-pointed, the point of intersection of the tangential lines will be the location of the leading edge determined by triangulation (cf. Mierla et al., 2009). From Fig. 3, it can be seen that these intersections (circled in red) occur outside the CME in both small and large propagation angle cases. For the large propagation angle regime (Fig. 3, left), the intersection occurs at an apparent propagation angle larger than the true propagation angle β, whereas for the small propagation angle regime, the apparent propagation angle is smaller.

To quantify the error using the thin hemispherical shell model, we make the additional simplifying assumptions that A and B are both at 1 AU, both in the ecliptic and at equal separations ($\pm\theta$ from Earth). The CME is assumed to propagate in the ecliptic plane and the calculation is only valid for the ecliptic plane. We further assume that all camera rays are parallel. As illustrated in Fig. 3, two cases must be considered in quantifying the systematic

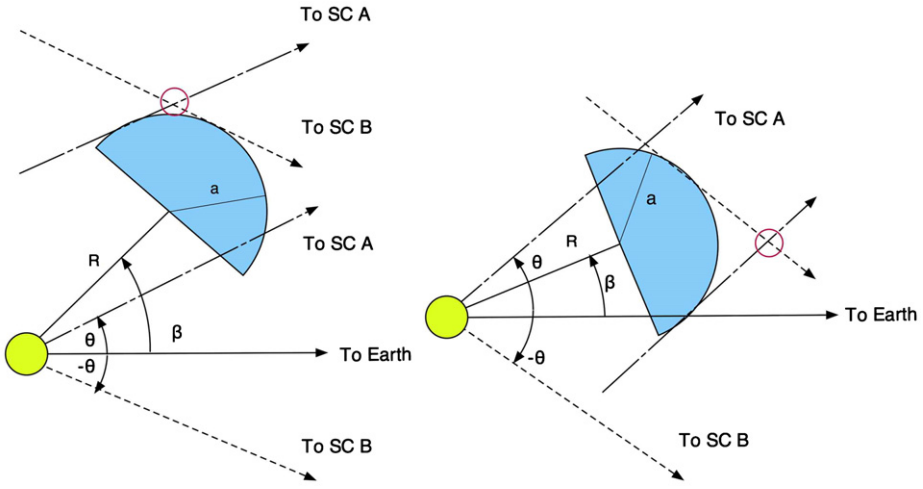

Fig. 3. Hemispherical shell model of CME propagating in the ecliptic plane at an angle β with respect to the Sun–Earth line; SC A(B) are located at θ ($-\theta$) from the Sun–Earth line. The density is in an infinitely thin layer on the surface of the hemisphere. The SC rays tangent to the hemisphere will have the largest line-of-sight integrated signal and produce the brightest feature; the tangent intersections are circled in red (see text). Left: Large propagation angle geometry $\beta>\theta$. Right: Small propagation angles $\beta<\theta$.

Please cite this article as: Liewer, P.C., et al., Stereoscopic analysis of STEREO/SECCHI data for CME trajectory determination. Journal of Atmospheric and Solar-Terrestrial Physics (2010), doi:10.1016/j.jastp.2010.09.004

error: the large ($\beta > \theta$, left) and small ($\beta < \theta$, right) propagation angle regimes. The error in the determination of both the propagation angle and the velocity is calculated in the Appendix. Here we give the expression relating β_{TT}, the propagation angle computed from T&T, with the true propagation angle β under the assumptions above. For the large propagation angle regime, we obtain

$$\tan\beta_{TT} = \frac{R\sin\beta + a/\cos\theta}{R\cos\beta} \quad (1)$$

For the small propagation angle regime, we obtain

$$\tan\beta_{TT} = \frac{R\sin\beta}{R\cos\beta + a/\sin\theta} \quad (2)$$

The error in the propagation longitude is defined as $\Delta_\beta = \beta_{TT} - \beta$; this error is plotted in Fig. 4 for both regimes for two values of the parameter a/R (see Fig. 3) for $\theta = 30^\circ$ (the DALE-effect errors vary slowly with θ). The upper (lower) curves apply in the large (small) propagation angle regime. From Fig. 4, it can be seen that for CMEs propagating in the ecliptic more than about 60°, but less than 120°, from the Sun–Earth line, the DALE-effect error in the propagation angle is less than 10°, going to zero for 90° from the Sun–Earth line. Note that for $\beta < 90^\circ$, the sign of the systematic error is such that the longitude determined by T&T is larger than the true propagation longitude (cf. Fig. 3, left); for $\beta > 90^\circ$, the error changes sign.

This analysis can also be used to obtain the systematic errors in location and velocity of the apex of the CME front. We define the fractional error in position as $\Delta_L/L = (L_{TT} - L)/L$ where L_{TT} is the position determined by T&T and L is the true distance from the Sun in the ecliptic plane, $L = a + R$ (see Fig. 3). Similarly we define the fractional error in velocity as $\Delta_V/V = (V_{TT} - V)/V$ where V is the true velocity of the front. Assuming that a/R remains constant as the CME propagates, it can be shown that the fractional error in velocity $\Delta_V/V = \Delta_L/L$. This error is derived (Eqs. (A1) and (A2)) and plotted in Appendix (Fig. A2). In the results below, we calculate the approximate DALE-effect errors in our determinations of the trajectory longitudes and velocities using these expressions.

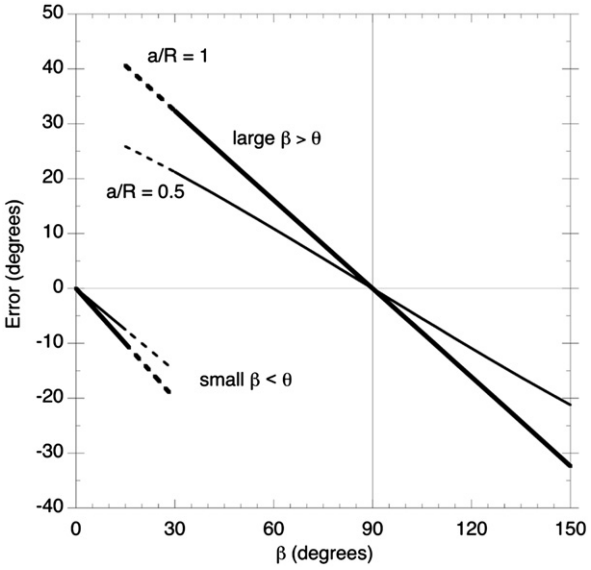

Fig. 4. Systematic error from the DALE effect in determination of CME propagation longitude. Upper curves are for the $\beta > \theta$ regime and the lower curves are for the small $\beta < \theta$ regime, where θ is the angle between the leading spacecraft and Earth. The calculation is for the ecliptic plane for $\theta = 30^\circ$.

In the small propagation angle regime, it can be seen from Fig. 4 that the DALE-effect errors in propagation angle are small, going to zero for propagation directly toward the observer. However, in Fig. 3 (right) the point of intersection lies significantly ahead of the CME front in this regime. From this (see also Fig. A2), it can be seen that errors in position and thus velocity for CMEs in the small propagation angle regime (which includes Earth-directed CMEs) can be quite large. Thus it is very important to take these errors into account when using T&T. Moreover such CMEs propagating near the Sun-observer line, where the Thomson scattering signal is weak, will be poorly defined in coronagraph images, making tie-pointing difficult.

From Figs. 3 and 4, it can be seen that the error increases significantly with a/R for this simple model. Note also that the error we calculate here depends on the assumption of a particular shape for the CME front; a different shape would give a different error. Thus the errors from the DALE effect given below should be considered estimates.

3. Results for determination of CME trajectories

The T&T technique has been used to determine the 3D trajectories of seven STEREO CMEs. Results are summarized in Table 1. The first column gives the date of the CME and, parenthetically below, the angle separating STEREO A and B. The velocity, latitude and longitude of the trajectory determined by T&T are given in column 2–4; the coordinates of the solar source region and its extent (not its uncertainty) are given parenthetically below the trajectory longitude and latitude. In an attempt to estimate the error in the trajectory from sources of error in tie-point placement other than the DALE effect (e.g. from effects discussed in Section 2.2), we include in columns 3 and 4 the standard deviation of the T&T trajectory direction: The trajectory direction is defined as the mean of the directions to the CME apexes at each reconstruction (each time) and the standard deviation is calculated relative to this mean. The errors in velocity and longitude estimated for the DALE effect are given in columns 5 and 6; these are computed assuming $a/R = 1$ using the spacecraft separation angle at the time of the CME using the equations in Section 2.3 and Appendix. The last three columns are the trajectory determined by TVH using forward modeling.

3.1. CME of 25 March 2008

Five leading edge reconstructions for the CME of 25 March 2008 were shown in Fig. 2. The resulting height time plot is shown in Fig. 5 where the height is the true height of the point on the leading edge most distant from the Sun (the apex). The velocity is obtained from a linear fit to the slope of the 3D height–time plot. The CME trajectory's latitude and longitude are the means of the latitudes and longitudes of the apex points from the five reconstructions. From these reconstructions, we obtained a propagation angle of -87° in longitude and -9° in latitude in the STYH coordinate system. The standard deviation of the directions to the apexes for these five reconstructions was $\delta_{STD} = \pm 2^\circ$ for both latitude and longitude. The estimated error in longitude from the DALE effect is, from Eq. (1) with $a/R = 1$, approximately -3°. The DALE-effect error in the velocity is, from Eq. (A1), $\Delta_V/V \approx 5\%$. These errors are small because the CME is propagating nearly perpendicular to the Earth–Sun line (cf. Fig. 4). For this viewing geometry, the error in direction from the DALE effect is comparable to the standard deviation. Both are small and the T&T trajectory determination should be very reliable.

For one check on the T&T trajectory determination, we compare the latitude and longitude of the trajectory to those of

Please cite this article as: Liewer, P.C., et al., Stereoscopic analysis of STEREO/SECCHI data for CME trajectory determination. Journal of Atmospheric and Solar-Terrestrial Physics (2010), doi:10.1016/j.jastp.2010.09.004

Table 1
Comparison of trajectory determinations and source region location and estimated error from DALE effect. See text for explanation.

	Results from T&T					Results from forward modeling—TVH Thernisien et al. (2009)		
	CME trajectory			Estimated error from DALE effect				
CME date (Separation angle AB)	V (km/s)	Longitude $\pm\delta_{STD}$ (STYH) (*source region & size*)	Latitude $\pm\delta_{STD}$ (STYH) (*source region*)	Error in V	Error in longitude	*V* (km/s)	Longitude STYH	Latitude STYH
8/31/2007 (28°)	313	$69^\circ\pm2^\circ$ (*flare ribbon* $63^\circ\pm4^\circ$)	$-20^\circ\pm5^\circ$ (*ribbon* $-17^\circ\pm7^\circ$)	2%	+10°			
11/16/2007 (40°)	383	$107^\circ\pm5^\circ$ (*filament* 99°)	$-20^\circ\pm5^\circ$ (*filament* −40°)	3%	−8°	350	123°	−15°
12/31/2007 COR1—LE	718	$-97^\circ\pm2^\circ$ (*PEA* $-100^\circ\pm4^\circ$)	$-9^\circ\pm5^\circ$ (*PEA* $-10^\circ\pm3^\circ$)	4%	+3°			
12/31/2007 CS dimple	753	$-92^\circ\pm2^\circ$	$-26^\circ\pm2^\circ$	4%	+1°			
12/31/2007 Upper lobe	819	$-89^\circ\pm1^\circ$	$-5^\circ\pm2^\circ$	4%	+1°	846	−91°	−5°
12/31/2007 Lower lobe	985	$-94^\circ\pm1^\circ$	$-51^\circ\pm2^\circ$	4%	+2°	967	−91°	−48°
1/02/2008 (44°)	619	$-64^\circ\pm7^\circ$ (*flare* $-68^\circ\pm2^\circ$)	$-5^\circ\pm4^\circ$ (*flare* $-4^\circ\pm3^\circ$)	3%	−13°	731	−51°	−9°
1/23/2008 (45°)	252	$-164^\circ\pm6^\circ$ (*backside*)	$-33^\circ\pm9^\circ$ (*backside*)	50%	−10°	442	−162°	−28°
3/25/2008 (47°)	1119	$-87^\circ\pm2^\circ$ (*PEA* $-80^\circ\pm4^\circ$)	$-9^\circ\pm2^\circ$ (*PEA* $-11^\circ\pm3^\circ$)	5%	-3°	1127	−84°	−12°
4/26/2008 (50°)	600	$-6^\circ\pm1^\circ$ (*flare ribbon* $-9^\circ\pm3^\circ$)	$1^\circ\pm1^\circ$ (*ribbon* $9^\circ\pm1^\circ$)	22%	+7°	741	−21°	6°

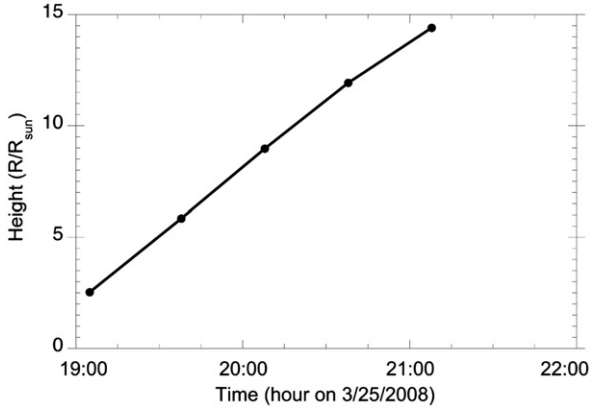

Fig. 5. True height–time profile for the CME of 25 March 2008 obtained from 3D reconstructions of the leading edge at five times. The earliest time was from COR1 data and the remainder from COR2 data, including that shown in Fig. 1.

the source region, since it is commonly assumed that, to a first approximation, CMEs propagate radially from the source region. (Deflection of the CME as it moves out through the strong fields of the lower corona is discussed later.) For this CME, the source region was determined as the location of a post-eruptive arcade (PEA); the PEA results from reconnection across the neutral line behind the CME and thus is a reliable indicator of the CME initiation site (see Cremedas and Bothmer, 2004 and references therein). At 19:56 UT, the PEA seen in EUVI 304 by STEREO B was centered in longitude at -80° (with an extent of $\pm4^\circ$) and in latitude at -11° (with an extent of $\pm3^\circ$). This is close to the longitude (-87°) and latitude (-9°) of the trajectory determined by T&T.

The T&T technique was validated by comparing CME trajectory results with those from a method that uses forward modeling to determine the 3D trajectory (TVH); this technique is not subject to the DALE effect. In TVH, the CME is modeled as a flux rope with a thin shell of density at the surface ("hollow croissant"). The size, height, orientation and propagation direction of the CME are chosen so that wireframe projections of the model CME, overlaid on the coronagraph images, agree best with the sequence STEREO A and B coronagraph image pairs. The iterative technique for determining the best fit trajectory parameters, described in TVH, uses visual inspection and a mathematical goodness of fit function. The velocity is determined in the same way as ours: by a linear fit to the CME apex height versus time data. The results from the TVH technique for velocity, longitude and latitude are given in the last three columns of Table 1. For the 25 March 2008 CME, the forward modeling technique results were in excellent agreement with the trajectory determined by T&T; the angles differed by 3° and the velocity to within 2%, within the estimated errors from the DALE effect and the standard deviation in the trajectory. The comparisons of the T&T trajectories with the TVH results and with the source region locations are also summarized graphically in Fig. 6.

3.2. CME of 31 December 2007

The T&T technique allows different parts of a CME to be tracked separately, e.g. the leading edge, the front edge of the dark cavity or the core, and a separate trajectory determined for each part. Here we illustrate this using the CME of 31 December 2007. The CME front had a normal, single-lobed structure in the COR1 field-of-view (FOV), but developed a two-lobed structure in the COR2 FOV (Fig. 7). Liu et al. (2009) interpret the dimple in the front as occurring where the CME is slowed as it plows through the denser solar wind at the heliospheric plasma sheet, whereas the upper and lower lobes are propagating into less dense, fast wind. The T&T technique was used to determine trajectories for four features: the single leading edge in the COR1 FOV and the three leading edge features in the COR2 FOV: upper lobe, lower lobe and dimple. In Fig. 7, the tie-points for the three COR2 features are shown on the COR2 images at 02:38 UT.

Fig. 8 shows the 3D reconstruction for all the features of the CME of 31 December 2007 at eight times from two viewpoints. The first three reconstructions used COR1 data from 1:05 to 01:15 with a 10 min cadence; the five reconstructions of the three COR2 features used data from 2:08 to 3:38 with 30 min cadence. On the left is a view in the solar equatorial plane; the view on the right is a polar view, looking down on the north pole of the Sun.

The trajectories of the COR1 front and the upper and lower lobes in COR2 were determined from the reconstructed leading edges shown in Fig. 8 as described above, e.g., using the point on the reconstructed leading edge most distant from the Sun at each time to give the height versus time curve, and averaging the longitudes and latitudes of those points to obtain the trajectory latitude and longitude. For the trajectory of the dimple, the point closest to the Sun at each time was used. Note that the longitude of the trajectory from the COR1 leading edge is -97° whereas the

Please cite this article as: Liewer, P.C., et al., Stereoscopic analysis of STEREO/SECCHI data for CME trajectory determination. Journal of Atmospheric and Solar-Terrestrial Physics (2010), doi:10.1016/j.jastp.2010.09.004

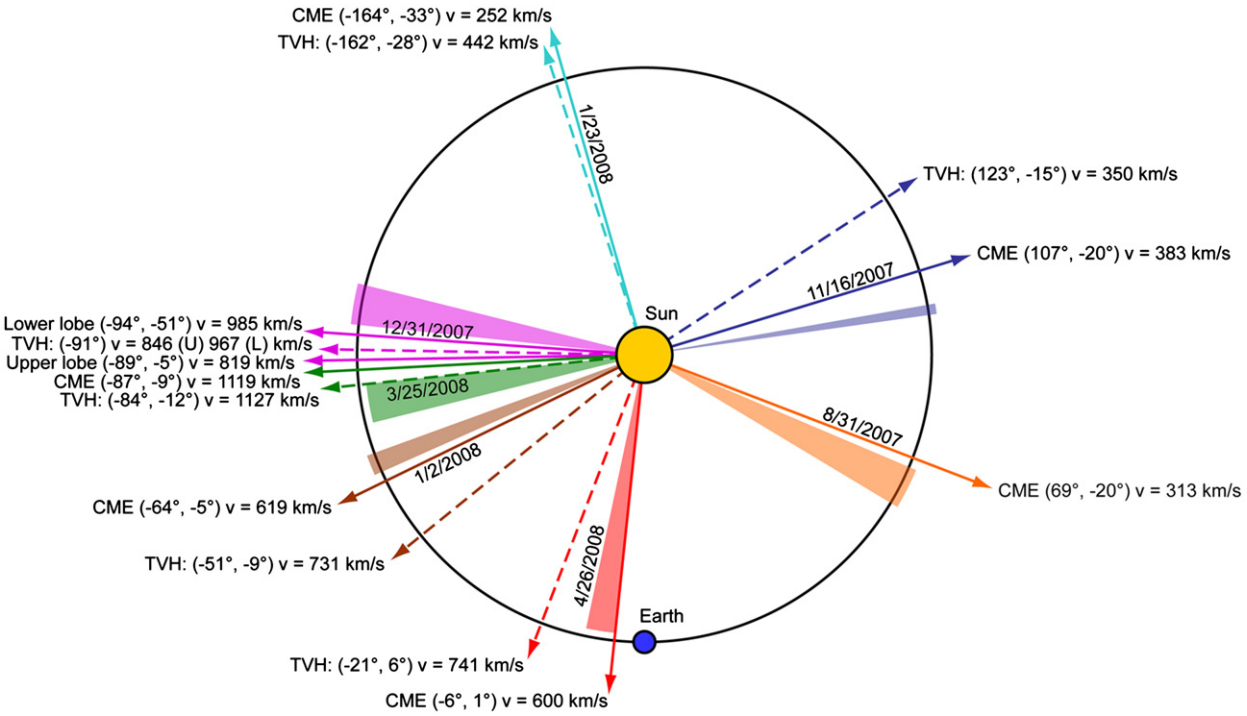

Fig. 6. Summary of 3D CME trajectories determined by T&T (solid arrows) and comparison with results from Thernisien et al. (2009) (TVH—dashed arrows) and with the longitude of the source regions (colored wedge).

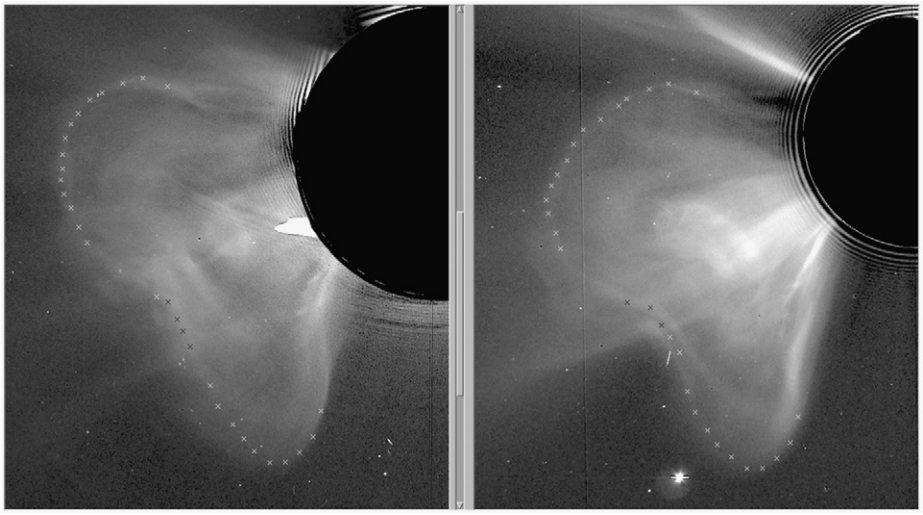

Fig. 7. Tie-point placement for three features of the front of the CME of 31 December 2007 at 02:38 UT. The COR2B (A) image on the left (right). The dimple and the upper and lower lobes were tracked separately.

longitudes of the COR2 features are -89° (upper lobe), -92° (dimple) and -94° (lower lobe). The four features were tracked separately and all four trajectories are given in Table 1. The standard deviations in the T&T trajectory determinations were quite small: $\delta_{STD} \sim 1$–2° in longitude and $\delta_{STD} \sim 2^\circ$ in latitude. The standard deviations are small because this fast, bright CME was very clearly imaged by both spacecraft; it was propagating nearly perpendicular to the Sun–Earth line and the spacecraft had a modest separation, making tie-point placement accurate. Approximate errors from the DALE effect (~ 1–2° in longitude, 4% in velocity) are also very small because of the nearly perpendicular propagation (cf. Fig. 4).

In Table 1, the trajectory determinations for the two lobes seen in COR2 are compared with those from the forward modeling of TVH, who used two flux ropes to model this structure. There is excellent agreement on the trajectories of the two lobes from the two techniques (within 3° for the longitude and latitude and within 3% in velocity which are comparable to the estimated errors from the DALE effect and, for longitude, the standard deviation as well).

The source region for this CME was clearly identifiable via the PEA. The source longitude was $-100^\circ \pm 4^\circ$, which is in good agreement with the COR1 CME longitude of -97°, but differs significantly from the longitudes of the three COR2 trajectories (-89° to -94°). This suggests that the CME has been deflected in longitude as it passed through the COR1 FOV. Inspection of the leading edge reconstructions of the COR1 segments at four times confirms this: the earliest reconstruction at 01:02 UT had a longitude of -98° (within the PEA

Please cite this article as: Liewer, P.C., et al., Stereoscopic analysis of STEREO/SECCHI data for CME trajectory determination. Journal of Atmospheric and Solar-Terrestrial Physics (2010), doi:10.1016/j.jastp.2010.09.004

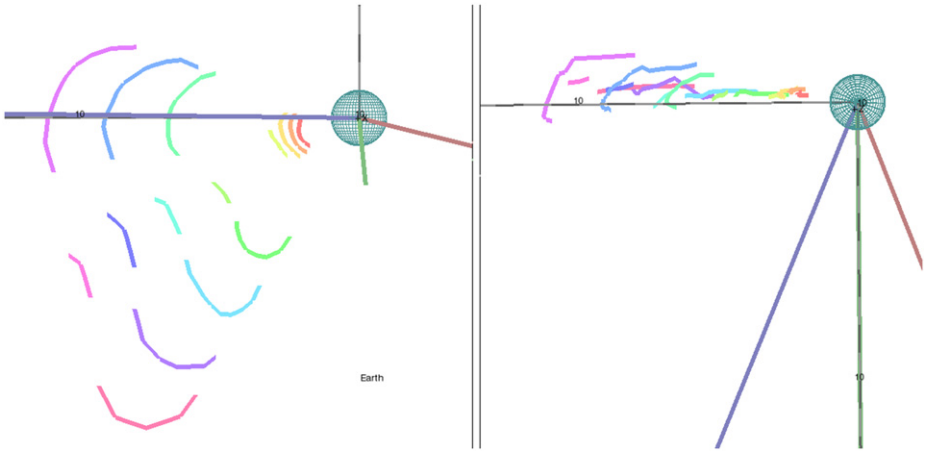

Fig. 8. Two views of 3D reconstructions of the leading edge of the CME of 31 December 2007 at eight times. The four line segments closest to the Sun (globe) are the reconstructions of the CME front in COR1 at four times. The outer segments are reconstructions from COR2 data for the two lobes and the dimple (see text). Left: View from a point in the solar equatorial plane. Right: View looking down on the north pole of the Sun.

source region of $-100^\circ \pm 4^\circ$ longitude) and the last reconstruction at 01:20 UT had a longitude of -94°. The overall deflection in longitude from the source region to the trajectory in COR2 is approximately 10°. This deflection is presumably due to the strong magnetic fields of the corona. While deflections in latitude have been well documented using LASCO observations (Cremedas and Bothmer, 2004), only with STEREO's two viewpoints can the deflections in longitude within the corona be observed.

3.3. CMEs of 16 November 2007

The two CMEs discussed above were propagating nearly perpendicular to Earth–Sun line where the error in propagation angle from the DALE effect is smallest (cf. Fig. 6). The trajectory longitude determined by T&T for the CME of 16 November 2007 indicates that this CME is propagating about 17° from perpendicular to the Sun–Earth line and the corresponding error in longitude (approximately -8°) from the DALE effect is somewhat larger than for the two CMEs discussed above (cf. Fig. 4). This trajectory was determined from seven reconstructions of the leading edge from COR2 observations (from 13:38 to 16:38 with a 30 min cadence) using the same procedure described above. The standard deviation in the T&T trajectory from these seven reconstructions was $\delta_{\mathrm{STD}} \sim 5^\circ$ for both angles.

No source region for the 16 November 2007 CME was visible on the solar disk from Earth or either spacecraft. This is not surprising: if the source were at the latitude and longitude of the trajectory, it would be behind the limb as viewed from Earth and STEREO B and at the limb for STEREO A. Nor could any obvious source region could be identified on the solar disk in the preceding day. A prominence eruption associate with this CME was visible, first, above the limb for STEREO A, and later, above the limb for STEREO B. The location of this prominence tip was determined by T&T using EUVI images at 08:45 UT, when visible by both spacecraft, and is given in Table 1. Its longitude (99°) is reasonably close to the longitude of the CME trajectory (107°). Note, however, since the tip of the erupting prominence may well have deviated in longitude from the source region, this determination of the source region is not as reliable as the other determinations based on on-disk signatures. The latitude of the source region (-40°) is considerably different from the latitude of the trajectory (-20°); the CME can be seen to deflect in latitude as it moves through the COR1 FOV (Liewer et al., 2009b).

The T&T trajectory is compared with that determined by TVH in Table 1 and Fig. 6, and, while the results for longitude are reasonably close (within $\sim 15^\circ$), the agreement is not as good as for the two CMEs propagating closer to the Sun–Earth line. Correcting for the approximately -8° error in longitude from the DALE effect brings the T&T angle to about $\sim 115^\circ \pm 5^\circ$, closer to the TVH longitude of 123°. The velocities from T&T and TVH are in very good agreement (within the 4% error expected from the DALE effect).

3.4. CME of 2 January 2008

The T&T trajectory for the CME of 2 January 2008 was determined from six reconstructions of the leading edge; three from COR1 (from 10:15 to 10:45 with a 15 min cadence) and three from COR2 observations (from 11:38 to 12:38 with a 30 min cadence). The standard deviation of the directions for these six reconstructions was $\delta_{\mathrm{STD}} \sim 4^\circ (7^\circ)$ in latitude (longitude). The trajectory longitude indicates that this CME is propagating -64° from Sun–Earth line, further from perpendicular than the three CMEs discussed above, and the corresponding DALE-effect error in longitude from Eq. (1) is larger (-13°) than for the more nearly perpendicular propagating CMEs; for this case, the DALE effect is apparently the dominant source of error. The source region location and extent was clearly identified by the accompanying flare and is given in Table 1 and Fig. 6; the source's location is within a few degrees of those of the T&T trajectory. The trajectory is compared with that determined by TVH in Table 1 and Fig. 6. The latitudes differ by only 4°; for comparison, the flare extended over 6° in latitude. The longitudes differ by 13° and the velocities by ~15%. In this case, correcting for the DALE-effect error in propagation angle brings the T&T and TVH longitudes into agreement at -51°. If this (-51°) is the correct trajectory longitude, then the CME has been deflected by about 17° from the source longitude ($-68^\circ \pm 2^\circ$). The velocities differ by ~15% which is larger than the approximate DALE-effect error (3%).

3.5. CME of 23 January 2008

Fig. 9 shows the CME of 23 January 2008 at 03:08 UT with the tie-points used for reconstruction; the image from COR1 A (B) is on the right (left). The CME front is more visible on a computer screen than in the image here, but, nevertheless, this figure illustrates the difficulty in placing tie-points on a CME front; the epipolar constraint is crucial. From this figure alone we know it is a backside CME: if it were heading toward B (left), then, in the COR1A image (right) it would appear to the left, not the right, of

Please cite this article as: Liewer, P.C., et al., Stereoscopic analysis of STEREO/SECCHI data for CME trajectory determination. Journal of Atmospheric and Solar-Terrestrial Physics (2010), doi:10.1016/j.jastp.2010.09.004

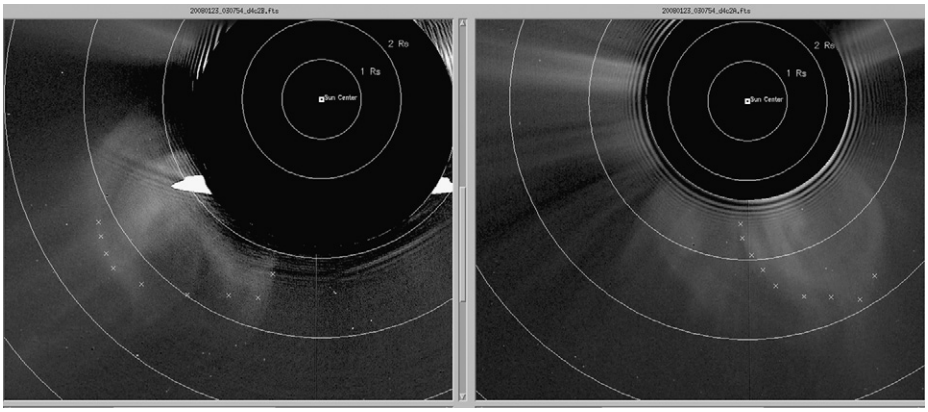

Fig. 9. CME of 23 January 2008 at 03:08 UT with tie-points. The COR1 A (B) image is on the right (left).

the center line. The T&T trajectory was determined from seven reconstructions, all in the COR2 FOV at 1:38, 2:08, then 4 from 3:08 to 4:38 at 30 min cadence, then 5:38). The standard deviation of the directions to the apex for these seven reconstructions was $\delta_{STD}\sim 9^\circ(6^\circ)$ in latitude (longitude). The longitude confirms that this is a backside CME, propagating -164° from the Sun–Earth line. This CME is in the small propagation angle regime for DALE-effect error since it is propagating 16° from the Earth–Sun line as extended behind the Sun. The error in longitude from the DALE effect (-10°) is comparable to the standard deviation. The propagation angle determined by T&T (-164°) is in excellent agreement with that determined by TVH (-162°), better agreement than expected from the above errors. The velocity disagreement, however, is significant (252 km/s vs. 442 km/s; see Table 1). This is consistent with the very large errors estimated for the DALE effect in this regime ($\Delta_V/V\sim 50\%$).

3.6. CME of 26 April 2008

The front of the 26 April 2008 CME was reconstructed at four times using COR2 observations from 17:08 to 18:38 at a 30 min cadence. The trajectory longitude determined from these reconstructions (-6°) puts this CME, like the previous case, in the small propagation angle regime for the DALE-effect error. The approximate DALE-effect error in longitude is relatively small (7°), but the DALE-effect error in velocity large (22%). The CME in the STEREO B images was seen as a partial halo; it was extremely faint and the tie-pointing difficult. Tie-pointing was only possible at four times over a relatively small range of distances (18–23 R_S). Fig. 10 shows a COR2 difference image for this CME at 18:38 UT with the STEREO A(B) image on the right (left). The standard deviation of the directions to the apex for the four reconstructions was very small, $\delta_{STD}\sim 1^\circ$ for both angles, much smaller than what one would expect considering the difficulty in placing the tie-points on this faint CME.

The source region longitude and extent, clearly identified by the flare ribbons, was $-9^\circ\pm 3^\circ$, which extends to the T&T longitude (-6°). The propagation longitude angle determined by TVH was -21°, close to STEREO B's longitude (-24°). This is not in agreement with the T&T longitude (-6°), although correcting for the estimated DALE-effect error brings the T&T longitude somewhat closer (to -13° compared to TVH's longitude of -21°). A detailed analysis, including forward modeling, of this CME by Wood and Howard (2009) concluded that the CME did hit STEREO B on 29 April 2008; they obtained a propagation longitude of -27°, close to the result obtained by TVH. Since the CME apparently did impact STEREO B, we conclude that the propagation angle is probably in the range -21° to -27°, as determined by TVH and Wood and Howard (2009), respectively, which differs from the T&T result by $\sim 10^\circ$ after applying the approximate DALE-effect error correction. This suggests that the T&T technique may be subject to significant ($>15^\circ$) errors for CMEs heading directly toward one of the spacecraft where the Thomson scattering signal is weakest and tie-point placement is difficult.

3.7. CME of 31 August 2007

The CME of 31 August 2007 was accompanied by a prominence eruption, which could be followed from the EUVI to the COR1 FOV. This CME front was reconstructed once using COR1 data at 22:05 and at eleven times using COR2 data (from 22:37 to 03:37 on 9/1/07 with a 30 min cadence). The trajectory determined from these reconstructions is given in Table 1 along with the estimated DALE-effect errors. The standard deviation of the directions to the apex for these seven reconstructions was $\delta_{STD}\sim 5^\circ(2^\circ)$ in latitude (longitude), compared to the 10° error in longitude from the DALE effect. The CME trajectory longitude and latitude as determined by the T&T technique are in agreement with the source longitude and latitude. This eruption will be the subject of a subsequent paper.

The results for the CMEs discussed in this section, summarized in Table 1 and Fig. 6, indicate that the T&T technique can be used to accurately determine CME trajectories (propagation angle and velocity) over a limited range of viewing geometries. This conclusion is based on the analysis of the error introduced by the DALE effect and by comparing T&T trajectories with those obtained by TVH using a forward modeling technique. For the CMEs propagating within a few degrees of perpendicular to the Sun–Earth line (31 December 2007 and 25 March 2008), both the direction and velocity were in excellent agreement with the trajectories determined by TVH; these also had the smallest calculated error from the DALE effect. The discrepancies between the two techniques became somewhat larger, but acceptable, as the propagation direction moved away from perpendicular to the Sun–Earth line, as expected from the DALE-error analysis of Section 2. For the CMEs propagating approximately 20–40° from perpendicular to Sun–Earth line, agreement with the TVH propagation trajectory was only fairly good, but agreement improved if corrections were made for the error from the DALE effect (within 10° for propagation angle and within 15% for velocity). For the CMEs propagating near the Sun–Earth line or its continuation beyond the Sun, while the trajectory angle was in fairly good agreement with TVH (within $\sim 15^\circ$), the agreement on velocity was poor as expected from the analysis of the DALE effect.

Please cite this article as: Liewer, P.C., et al., Stereoscopic analysis of STEREO/SECCHI data for CME trajectory determination. Journal of Atmospheric and Solar-Terrestrial Physics (2010), doi:10.1016/j.jastp.2010.09.004

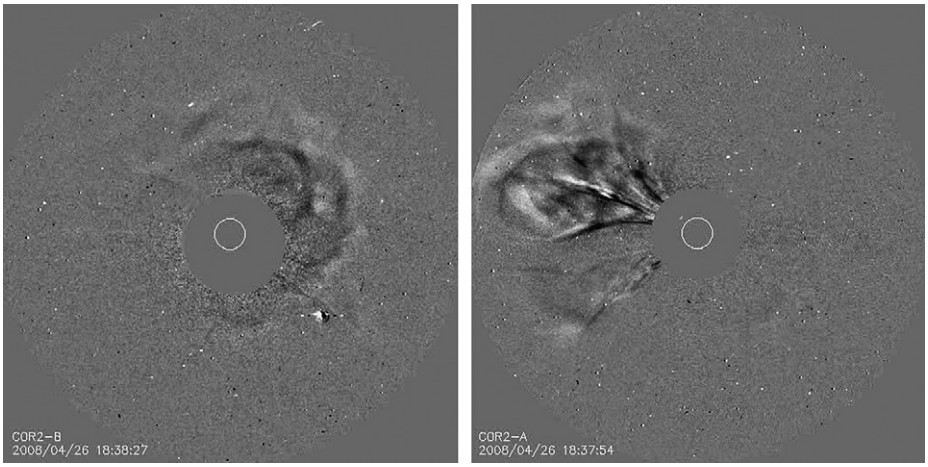

Fig. 10. Difference image of the 26 April 2008 CME at 18:38. The CME in the STEREO B image appears as a partial halo (Courtesy of S. Plunkett).

4. Comparison of trajectory with HI1 observations

It is difficult to extend the tie-pointing technique into STEREO's heliospheric imagers FOVs because the CME front is generally only seen clearly in the images from one spacecraft. Here we discuss a method for using the CME track (angle from the Sun as a function of time) as observed by just one of the STEREO spacecraft to verify the 3D trajectory determined from the coronagraphs and also to study the evolution of the CME trajectory beyond the coronagraph's FOV. This technique is based on the work of Sheeley et al. (1999) (see also Rouillard et al., 2008) who showed that for a CME (or any solar wind transient) moving radially at a constant velocity, there is a unique relationship between the elongation (angle from the Sun) as a function of time, the propagation angle ϕ with respect to the observer and the radial velocity V:

$$\alpha(t) = \arctan\left[\frac{V(t-t_0)\sin\phi}{R_O - V(t-t_0)\cos\phi}\right], \quad (3)$$

where $\alpha(t)$ is the elongation angle, R_O is the distance to the observing spacecraft, and t_0 is determined by $\alpha(t_0)=0$. Thus, a plot of elongation versus time for a constant velocity CME moving radially is not a straight line (as it would be for a narrow angle coronagraph FOV), but rather it can curve upward (small ϕ—apparent acceleration) or downward (large ϕ—apparent deceleration). For coronagraphs with narrow FOVs, plots of elongation versus time are often shown as "height versus time" plots, which shows the height projected on the plane-of-sky; acceleration or deceleration is readily apparent from the curvature of the height–time plot. In the HI FOVs, one cannot determine whether a CME is accelerating or decelerating without knowing the propagation angle ϕ. The propagation angle ϕ in Eq. (3) is measured in the plane containing the observer (STEREO A or B) and the CME propagation vector.

The relationship between the elongation versus time and a transient's trajectory (Eq. (3)) has been used to determine the propagation angle from observed elongation versus time plots (Davies et al., 2009). This technique uses data from only one spacecraft and thus is not subject to errors from the DALE effect; it does however assume that the same feature is tracked through the heliospheric imager's FOV and thus it is subject to errors from Thomson sphere effects. Here, we use this relationship, in conjunction with HI1A or B observations, to verify the CME trajectories determined by T&T from the coronagraph data: The $\alpha(t)$ predicted by Eq. (3) for the HI1 FOV using CME trajectory parameters (velocity and propagation angle) determined by T&T

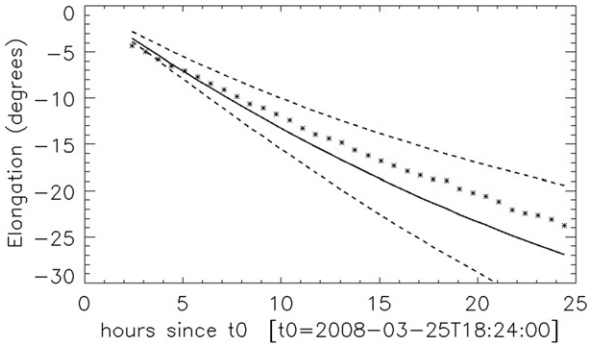

Fig. 11. Comparison of measured and predicted $\alpha(t)$ curves for the CME of 25 March 2008, observed by HI1 A on 26 March. The asterisks are elongations measured from the HI A images. The solid line is the predicted $\alpha(t)$ using the trajectory parameters obtained from T&T (Table 1). The dashed lines show the predicted trajectory for $\pm 20^\circ$ in the T&T propagation angle.

should agree with the $\alpha(t)$ measured for the CME in HI1, at least near the inner edge of the HI1 FOV. We obtain the elongation $\alpha(t)$ by tracking the leading edge of the CME at the position angle corresponding to the latitude of the T&T trajectory in a sequence of HI1 difference images from a single spacecraft (An or B). We then compare this $\alpha(t)$ with the predicted $\alpha(t)$ track from Eq. (3) using the velocity and CME propagation angle obtained from T&T. The propagation angle ϕ in Eq. (3) is measured in the plane containing the observer and the CME propagation vector (Rouillard et al., 2009); this must be accounted when calculating ϕ in Eq. (3) from the STYH latitude and longitude of the trajectory.

The leading edge of the CME of 25 March 2008, propagating at -87° longitude and -9° latitude as found by the T&T technique, was easily tracked in the HI1-A field of view. We tracked the leading edge of the CME as seen in a sequence of HI1A different images at the position angle of the latitude of the T&T trajectory using routines in the SECCHI SolarSoft library (`scc_mkmovie` and `scc_wrunmoviem`). Fig. 11 compares the observed $\alpha(t)$ versus t measured from HI A images (asterisks) with the predicted $\alpha(t)$ versus t calculated from Eq. (3); negative elongations correspond to propagation to the left of the Earth–Sun line. The solid line is the predicted $\alpha(t)$ from Eq. (3) using the trajectory parameters in Table 1 and the R_O for STEREO A. To help estimate the agreement or disagreement between observed and predicted, we also plot as dashed lines the predicted trajectories for $\pm 20^\circ$ in propagation longitude. For this case, there is excellent agreement between the observed and predicted curves at early times, confirming the

Please cite this article as: Liewer, P.C., et al., Stereoscopic analysis of STEREO/SECCHI data for CME trajectory determination. Journal of Atmospheric and Solar-Terrestrial Physics (2010), doi:10.1016/j.jastp.2010.09.004

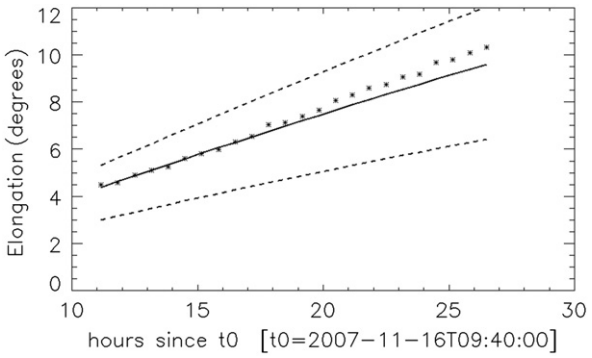

Fig. 12. Comparison of measured and predicted elongation versus time curves for the CME of 16 November 2007. The asterisks are elongations measured from the HI1B images. The solid line is the predicted trajectory using the trajectory parameters obtained from T&T (Table 1). The dashed lines show the predicted trajectory for $\pm 20^\circ$ in the T&T propagation angle.

trajectory from T&T (and TVH—see discussion in Section 3). At later times, the measured elongation lags the prediction, suggesting that the CME has decelerated; this is probably due to the interaction of this fast CME (1119 km/s) with slow solar wind. Other interpretations are also possible, e.g., the CME propagation angle changed, the shape changed, or the Thomson scattering effects modified the appearance or what portion of the CME was being tracked.

The CME of 16 November 2007 could be easily tracked in the HI1B observations. As in the above case, the bright leading edge was tracked at the position angle corresponding to the latitude of the trajectory (-20°) in a sequence of HI1B difference images to give an observed track $\alpha(t)$ as a function of time. The predicted track in the HI1B field-of-view was calculated from Eq. (3) using the trajectory parameters determined from the coronagraph data (Table 1). Fig. 12 compares the observed and elongation versus time plots. The solid line is the predicted $\alpha(t)$ from Eq. (3) using the trajectory parameters in Table 1 and the R_O for STEREO B; the dashed lines again show, for reference only, the predicted trajectory for $\pm 20^\circ$ in the propagation angle longitude. For this case, the agreement is again excellent at early times, confirming the T&T trajectory, which, for this case, differed from the trajectory determined by TVH by about 15° in longitude. Here, the observed track $\alpha(t)$ leads the prediction slightly at later times, suggesting an acceleration, possibly by the interaction of this slow CME (383 km/s) with faster solar wind.

We note that the technique used here is similar to that used by Maloney et al. (2009) to study CME propagation beyond COR2: after determining the trajectory from stereoscopic analysis of the STEREO coronagraph data, they also assumed the CME continued to propagate in the same direction (“pseudo-radially”) and used observations from the heliospheric imagers to determine the velocity.

5. Summary and conclusions

The STEREO mission with its twin spacecraft has given us the first chance to use stereoscopic data analysis techniques on solar images. In this paper, we have discussed the application of the technique of tie-pointing and triangulation (T&T) to white light images of CMEs. What is seen as the bright leading edge in a white light image of a CME is the result of the line-of-sight integration through the CME. Two different apparent leading edges are seen from the two viewpoints of the separated spacecraft (the DALE effect), and tie-pointing these two different leading edges leads to a systematic error in reconstructing the leading edge by triangulation.

Here, we have used T&T to determine the trajectories of seven STEREO CMEs using time sequences of A and B coronagraph images and calculated an approximate error from the DALE effect. This error was analyzed using a simple thin hemispherical shell model of a CME front. To validate the use of T&T on CME trajectory determination and the DALE-effect error analysis, we compared results with those from the forward-modeling technique of TVH that is not subject to the DALE effect and with the locations of the solar source regions. The results were summarized in Table 1 and Fig. 6.

The results indicate that the T&T technique can be used to accurately determine CME trajectories (propagation angle and velocity) for CMEs propagating within roughly $\pm 40^\circ$ of perpendicular to Sun–Earth line for the range of spacecraft separations studied ($\leq 50^\circ$). Within this range, T&T and TVH agreed reasonably well (within 10° for propagation angle and within 15% for velocity). Excellent agreement (a few degrees in direction and few percent in velocity) with TVH was obtained for CMEs propagating within 10° of perpendicular to the Sun–Earth line. We found that the accuracy generally degraded slowly as the propagation direction moves away from nearly perpendicular, and allowances need to be made for the error from the DALE effect. The T&T techniques appears somewhat unreliable for CMEs propagating within $\pm 20^\circ$ of the Sun–Earth line. For these CMEs, although the direction is in reasonable agreement with TVH, the agreement on velocity was poor as expected from the analysis of the DALE effect. For the backside CME propagating 15° from the extended Sun–Earth line, we obtained excellent agreement for the propagation angle with the TVH technique, but a large ($\sim$50%) discrepancy in velocity, which is consistent with the error from the DALE effect. For the front-side CME near the Sun–Earth line, the velocity discrepancy (23%) was again consistent with the DALE-effect error. For this case, the T&T and TVH angles differed by 11° even after correcting for the DALE-effect error.

Comparison of the trajectory latitudes with those of the source regions shows significant deflection in several cases; deflection in latitude by the strong coronal fields of the low corona is a well-documented phenomenon (see Cremedas and Bothmer, 2004 and references therein). In one case presented here, the CME of 31 December 2007, we are also able to measure deflection in longitude within the coronagraphs' FOVs.

In this paper, we also use the CME observations in the HI1 FOV to verify the trajectory determined by T&T in the coronagraph FOV and to study the propagation beyond the coronagraph FOVs for two CMEs with well-determined trajectories, 26 March 2008 and 16 November 2007. CMEs moving radially with a constant velocity have a unique track in elongation versus time plots in the heliospheric imager FOVs, and if the observed and predicted tracks agree at early times in the HI1 data, then the trajectory is confirmed. In both cases, the agreement was excellent; later deviations from the predicted track may indicate acceleration or deceleration as the CME moves through the heliosphere. However, other interpretations are also possible because of the different appearance of the CME in the FOV of the heliospheric images, due to evolution and to Thomson scattering effects.

In conclusion, for the range of spacecraft separations studied, the T&T technique can be used reliably to determine CME trajectories over a limited range of viewing geometries. The range can be increased if allowances are made for the error introduced by the DALE effect. These errors can be large, depending on the viewing geometry and the direction of propagation of the CME. T&T technique can also be used to track other features (cavity edge, core) to study how the relationship of these features evolves as the CME propagates. The technique could also be used to

Please cite this article as: Liewer, P.C., et al., Stereoscopic analysis of STEREO/SECCHI data for CME trajectory determination. Journal of Atmospheric and Solar-Terrestrial Physics (2010), doi:10.1016/j.jastp.2010.09.004

measure expansion, both in radius and latitude as the CME propagates through the coronagraph FOVs. The software tools (`Sunloop` and the viewer `Animator`) are available in the SECCHI SolarSoft library.

Acknowledgments

We thank A. Vourlidas and S. Plunkett for useful discussions. We thank N. Rich and S. Suzuki for their help with the SECCHI data. The *STEREO*/SECCHI data used here are produced by an international consortium of the Naval Research Laboratory (USA), Lockheed–Martin Solar and Astrophysics Lab (USA), NASA Goddard Space Flight Center (USA), Rutherford Appleton Laboratory (UK), University of Birmingham (UK), Max-Planck-Institut für Sonnensystemforschung (Germany), Center Spatiale de Liege (Belgium), Institut d'Optique Théorique et Appliqueé (France), Institut d'Astrophysique Spatiale (France). The USA institutions were funded by NASA; the UK institutions by Particle Physics and Astronomy Research Council (PPARC); the German institutions by Deutsches Zentrum für Luft- und Raumfahrt e.V. (DLR); the Belgian institutions by Belgian Science Policy Office; the French institutions by Center National d'Etudes Spatiales (CNES) and the Center National de la Recherche Scientifique (CNRS). The NRL effort was also supported by the USAF Space Test Program and the Office of Naval Research. A portion of this work was carried out at the Jet Propulsion Laboratory, California Institute of Technology under a contract with NASA.

Appendix. Calculation of systematic error

As discussed in Section 2.3, a systematic error in the determination of a CME trajectory using tie-pointing and triangulation (T&T) results from the fact that the apparent CME bright leading edge results from the line-of-sight integrated signal through an optically thin medium. Different apparent leading edges are seen and tie-pointed (the DALE effect), leading to an error in the reconstruction by triangulation. Here we derive the expressions for the DALE-effect errors in propagation longitude and velocity given in Section 2.3, calculated using the simple thin hemispherical CME model introduced in Section 2 and Fig. 3. We make the simplifying assumptions that the leading and trailing spacecraft (A and B) are both at 1 AU, in the ecliptic, and at equal separations ($\pm\theta$ from Earth). All are very good assumptions for STEREO CMEs studied here. We also assume that the lines tangent to the shell (the lines with the largest integrated signal for the model) are parallel to the direction to the spacecraft. The calculation is done for CMEs propagating in the ecliptic plane and is only valid in the ecliptic plane. There are two different regimes of errors for large ($\beta > \theta$) and small ($\beta < \theta$) propagation angles, where β is the propagation angle of the CME relative to Earth, as illustrated in Fig. 3.

Fig. A1 shows the geometry used in the calculation of the error in the large propagation angle regime, $\beta > \theta$. In Fig. A1, the

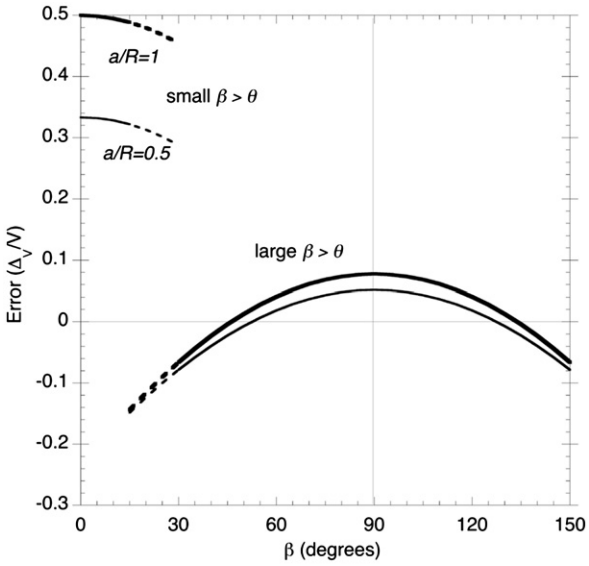

Fig. A2. Systematic error in determination of CME velocity from the DALE effect for thin shell model of Fig. 3 for two ratios of *a/R*. The lower curves apply in the large $\beta > \theta$ regime and the upper curves in the small $\beta < \theta$ regime where θ is the angle between the leading spacecraft and Earth. The calculation is for the ecliptic plane for $\theta = 30^\circ$.

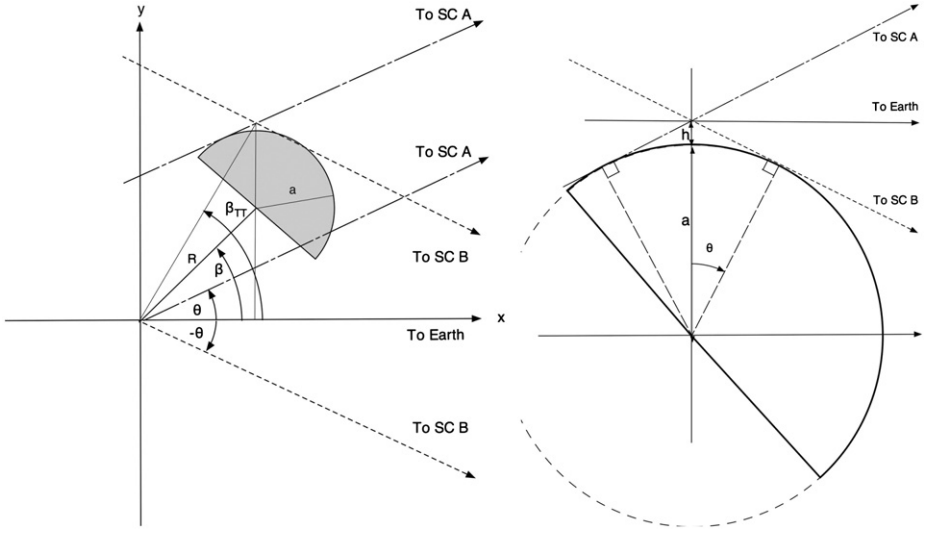

Fig. A1. Left: Geometry for a hemispherical model CME propagating at an angle β with respect to Earth for the case $\beta > \theta$. The tie-pointing and triangulation technique will determine the bright leading edge to be at the point of intersection of the lines tangent to the hemisphere. Right: Detailed geometry to determine *h*, the height of the tangent intersection point above the hemisphere.

Please cite this article as: Liewer, P.C., et al., Stereoscopic analysis of STEREO/SECCHI data for CME trajectory determination. Journal of Atmospheric and Solar-Terrestrial Physics (2010), doi:10.1016/j.jastp.2010.09.004

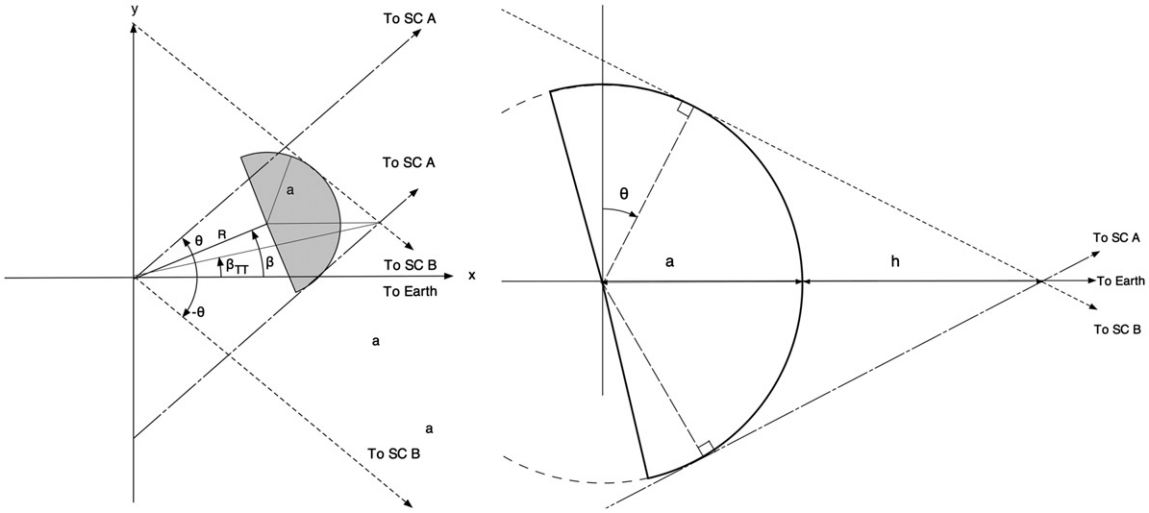

Fig. A3. Left: Geometry for a hemispherical model CME propagating at an angle β with respect to Earth for the case $\beta < \theta$. The tie-pointing and triangulation technique will determine the bright leading edge to be at the point of intersection of the lines tangent to the hemisphere. Right: Detailed geometry to determine h, the height of the tangent intersection point ahead of the hemisphere.

directions to the A (dashed dotted lines) and B (dashed lines) spacecraft and the tangent lines are labeled. In the ecliptic plane, the tangent lines intersect outside the CME and cause β_{TT}, the propagation angle determined by T&T, to be larger than the true propagation angle β. The intersection falls on a line through the sphere center perpendicular to the direction to Earth because of the equal separation assumption; the x coordinate of this line is $x=R\cos\beta$ where R is the distance of the sphere center from the Sun. The expanded view on the right side of the figure shows the geometry used to compute the height h above the CME of this intersection point needed to obtain the y coordinate of the intersection. This height is given by $h=a\,(1-\cos\theta)/\cos\theta$, yielding $y=R\sin\beta+a+h=R\sin\beta+a/\cos\theta$. This yields the relationship between the true propagation angle β and the propagation angle from the T&T technique β_{TT} given in Section 2.3 (Eq. (1)) and plotted in Fig. 4 for $a/R=0.5$ and 1.0 for $\theta=30^\circ$.

The DALE-effect error in position can be found by comparing the true location of the leading edge $L=R+a$ with the distance to the intersection point L_{TT}, where $L_{TT}^2=x^2+y^2$. The result for the fractional error is

$$\frac{\Delta_V}{V}\equiv\frac{\Delta_L}{L}=\frac{L_{TT}-L}{L}=\frac{\sqrt{1+2a\sin\beta/R\cos\theta+a^2/(R\cos\theta)^2}}{1+a/R}-1 \qquad \text{(A1)}$$

As discussed in the text, the fractional error in position L and velocity of the front are identically equal assuming a/R remains constant as the CME propagates. This fractional error is plotted in Fig. A2 for $a/R=0.5$ and 1.0 for $\theta=30^\circ$; the lower curves are for the large propagation angle regime. Note that the error goes through zero at about 50° and 130°, which gives rise to the small systematic errors in velocity appearing in Table 1.

Fig. A3 shows the geometry used to find the error for the small propagation angle regime, $\beta<\theta$. In this case, the tangent intersection is closer to Earth than the actual CME apex and the intersecting tangents are from opposite sides of the CME. For this geometry, the coordinates of the intersection are $x=R\cos\beta+a/\sin\theta$ and $y=R\sin\beta$, yielding the relationship between the observed and true propagation angle given in Section 2.3, Eq. (2) (also plotted in Fig. 4),

$$\tan\beta_{TT}=R\sin\beta/(R\cos\beta+a/\sin\theta)$$

For this regime, the fractional error in position and velocity is given by

$$\frac{\Delta_V}{V}\equiv\frac{\Delta_L}{L}=\frac{L_{TT}-L}{L}=\frac{\sqrt{1+2a\cos\beta/R\sin\theta+a^2/(R\sin\theta)^2}}{1+a/R}-1 \qquad \text{(A2)}$$

This fractional error is plotted in Fig. A2 for $a/R=0.5$ and 1.0 and $\theta=30^\circ$; the upper curves are for the small propagation angle regime. Note that the errors in position and velocity are quite large in this regime, which gives rise to the large DALE-effect errors in velocity appearing in Table 1. Thus it is important to make allowance for these errors to use the T&T technique for space weather prediction.

References

Aschwanden, M.J., Wuelser, J.-P., Nitta, N., Lemen, J., 2008. Astrophys. J. 680, 1477.
Baker, D., 2000. JASTP 62, 1669. doi:10.1016/S1364-6826(00)00119-X.
Billings, D.E., 1966. A Guide to the Solar Corona. Academic Press, New York.
Cremedas, H., Bothmer, V., 2004. Astron. Astrophys. 422, 307.
Colaninno, R., Vourlidas, A., 2009. Astrophys. J. 698, 852.
Davies, J.A., Harrison, R.A., Rouillard, A.P., Sheeley, N.R., Perry, C.H., Bewsher, D., Davis, C.J., Eyles, C.J., Crothers, S.R., Brown, D.S., 2009. GRL 36, L02102.
Feng, L., Inhester, B., Solanki, S.K., Wiegelmann, T., Podlipnik, B., Howard, R.A., Wuelser, J.-P., 2007. Astrophys. J. 671, L205–L208.
Howard, R.A., Moses, J.D., Vourlidas, A., Newmark, J.S., Socker, D.G., Plunkett, S.P., Korendyke, C.M., Cook, J.W., Hurley, A., Davila, J.M., et al., 2007. Space Sci. Rev. 136, 67.
Hundhausen, A.J., 1993. J. Geophys. Res. 98, 13177.
Inhester, B., 2006. Stereoscopy basics for the STEREO mission, eprint arXiv:astro-ph/0612649 (to appear as a Publ. of the Int. Space Sci. Inst.).
Kaiser, M., 2005. Adv. Space Res. 36, 1483.
Liewer, P.C., De Jong, E.M., Hall, J.R., Howard, R.A., Thompson, W.T., Culhane, J.L., Bone, L.A., Van Driel-Gesztelyi, L., 2009a. Sol. Phys. 256, 57.
Liewer, P.C., De Jong, E.M., Hall, J.R., Howard, R.A., Thompson, W.T., 2009b. Determination of CME trajectories by stereoscopic analysis of STEREO/SECCHI data. In: Twelfth International Solar Wind Conference, AIP Conference Proceedings, 2010, p. 412.
Liu, Y., Luhmann, J.G., Lin, R.P., Bale, S.D., Vourlidas, A., Petrie, G.J.D., 2009. Astrophys. J. 698, L51.
Luhman, J.G., 1997. Coronal Mass Ejections, AGU Geophysical Monograph 99, 291.
Maloney, S., Gallagher, P.T., McAteer, R.T.J., 2009. Sol. Phys. 256, 149.
Mierla, M., Davila, J., Thompson, W., Inhester, B., Srivastava, N., Kramar St., M., Cyr, O.C., Stenborg, G., Howard, R.A., 2008. Sol. Phys. 252, 385.
Mierla, M., Inhester, B., Marque, C., Rodriguez, L., Gissot, S., Zhukov, A., Berghmans, D., Davila, J., 2009. Sol. Phys. 259, 123.
Mierla, M., Inhester, B., Antunes, A., Boursier, Y., Byrne, J.P., Colaninno, R., Davila, J., deKoning, C.A., Gallager, P.T., Gissot, S., et al., 2010. Ann. Geophys. 28, 203.

Please cite this article as: Liewer, P.C., et al., Stereoscopic analysis of STEREO/SECCHI data for CME trajectory determination. Journal of Atmospheric and Solar-Terrestrial Physics (2010), doi:10.1016/j.jastp.2010.09.004

Rouillard, A.P., Davies, J.A., Forsyth, R.J., Rees, A., Davis, C.J., Harrison, R.A., Lockwood, M., Bewsher, D., Crothers, S.R., Eyles, C.J., 2 coauthors, 2008. Geophys. Res. Lett. 35, L10110.
Rouillard, A.P., Savani, N.P., Davies, J.A., Lavraud, B., Forsyth, R.J., Morley, S.K., Opitz, A., Sheeley, N.R., Burlaga, L.F., Sauvaud, J.-A., 10 coauthors, 2009. Sol. Phys. 256, 307.
Sheeley Jr., N.R., Walters, J.H., Wang, Y.-M., Howard, R.A., 1999. J. Geophys. Res. 104, 24739.
Srivastava, N., Venkatakrishnan, P., 2004. J. Geophys. Res. 109. doi:10.1029/2003JA010175 CiteID A10103.
Srivastava, N., Inhester, B., Mierla, M., Podlipnik, B., 2009. Sol. Phys. 259, 213.
Temmer, M., Preiss, S., Veronig, A.M., 2009. Sol. Phys. 256, 183.
Thernisien, A., Vourlidas, A., Howard, R.A., 2009. Sol. Phys. 256, 111.
Thompson, W.T., 2006. Astron. Astrophys. 449, 791.
Vourlidas, A., Howard, R.A., 2006. Astrophys. J. 642, 1216.
Wood, B.E., Howard, R.A., 2009. Astrophys. J. 702, 901.

Please cite this article as: Liewer, P.C., et al., Stereoscopic analysis of STEREO/SECCHI data for CME trajectory determination. Journal of Atmospheric and Solar-Terrestrial Physics (2010), doi:10.1016/j.jastp.2010.09.004